continued including the nonhydrogen atoms from these diethyl ether molecules and the hydrogen atoms of the palladium dimers.[18] Refinement converged to $R = 0.062$ and $R_w = 0.056$.

Acknowledgment. We thank the Division of Basic Chemical Sciences of the Department of Energy for support of this work. We thank Phillips Petroleum Co. for a summer stipend to U.B. We thank Professors J. P. Hunt and R. E. Hamm for helpful discussions on kinetics. Structural data were collected by Mr. D. Bloomquist, and Professor R. D. Willett gave some assistance with the structure solution. Thanks are due to the National Science Foundation for funds to purchase the Bruker WH90 NMR spectrometer (Grant No. 75-06301). Data on the Bruker WH90 were collected by Mr. D. Appel. We thank Professor R. Eisenberg for communication of his results on mixed sulfur–selenium ligands and Professor J. A. Ibers for a copy of his HYDRA program.

(18) The hydrogen positions were calculated by using the HYDRA program.

Registry No. *o*-$MeSC_6H_4PPh_2$, 14791-94-7; $Pd(SCN)_2$(*o*-$MeSC_6H_4PPh_2$), 30482-42-9; PdI_2(*o*-$MeSC_6H_4PPh_2$), 28647-06-5; $Pt(SMe)_2(PPh_3)_2$, 56213-50-4; $RuCl_2$(*o*-$MeSC_6H_4PPh_2)_2$, 74449-46-0; *o*-$MeSeC_6H_4PPh_2$, 16566-17-9; $Pd(SCN)_2$(*o*-$MeSeC_6H_4PPh_2$), 30482-43-0; *o*-$MeSeC_6H_4SMe$, 74449-35-7; $PdCl_2$(*o*-$MeSeC_6H_4SMe$), 74449-47-1; $PdCl_2$(*o*-$Me_2NC_6H_4PPh_2$), 14552-56-8; [PdI(*o*-$SC_6H_4PPh_2$)]$_2$, 52543-13-2; [PdI_2(*o*-$SC_6H_4PPh_2$)]$^-$, 71763-87-6; SCN^-, 302-04-5; I^-, 20461-54-5; *o*-$BrSeC_6H_4SMe$, 74449-36-8; K_2PdCl_4, 10025-99-7; Na_2PdCl_4, 10026-00-3; $RuCl_2$(*o*-$MeSeC_6H_4PPh_2)_2$, 74465-44-4.

Supplementary Material Available: A listing of observed and calculated structure factors (19 pages). Ordering information is given on any current masthead page.

Contribution from the Departments of Chemistry, University of North Dakota, Grand Forks, North Dakota 58202, and University of Houston, Houston, Texas 77004

Structure of (η^6-Mesitylene)bis(pentafluorophenyl)nickel(II). Analysis of the Bonding in Arene–ML_2 Complexes

LEWIS J. RADONOVICH,*[1a] FRANKLIN J. KOCH,[1a] and THOMAS A. ALBRIGHT*[1b,c]

Received April 15, 1980

The compound (η^6-mesitylene)bis(pentafluorophenyl)nickel(II) crystallizes in space group $P2_1/n$ with lattice constants of $a = 8.556$ (1) Å, $b = 19.125$ (3) Å, $c = 12.135$ (3) Å, and $\beta = 86.60$ (2)°. The structure was determined from 3279 observed data in the range $(\sin\theta)/\lambda \leq 0.648$ Å^{-1}. The average Ni–C_6F_5 bond distance was 1.898 (4) Å, and the average Ni–C_π bond distance was 2.211 (4) Å. A small "boat" type deformation of the carbon framework in the η^6-mesitylene ligand is observed. Extended Hückel calculations on molecules of the type (benzene)ML_2 reveal that the M–arene distance and deformation of the arene from planarity vary in a predictable manner as a function of the electron count. The 16-electron complexes remain planar and have shorter M–arene distances compared to the 18-electron analogues. This analysis is extended to (arene)ML_4 and other species.

Introduction

Previously we reported[2,3] the synthesis and structures of (π-tol)$M(C_6F_5)_2$ complexes where M = Co(II) and Ni(II). An interesting feature of these molecules is that the π-arene ligand is extremely labile. For example, the solution data indicates that the arene rapidly undergoes exchange at room temperature, with the more electron-releasing arenes being preferred. Other arene complexes normally require much more forcing conditions or a catalyst.[4] Herein we report the structure of the π-mesitylene complex of $(C_6F_5)_2Ni$ (**1**) to

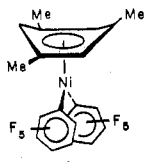

1

establish the structural changes that occur when the more electron-releasing mesitylene is substituted for toluene and also to provide more structural data on complexes of this type. Moreover, we wish to develop an understanding of the bonding in arene–ML_2 complexes. Of particular interest is the fact that the π-arene ligand is sometimes nonplanar. This is, of course, the case for η^4 and η^2 complexes.[5] However, we have observed[3b] that the complex (π-tol)$Ni(C_6F_5)_2$ contains a nonplanar ring which has also been observed in other[6] 18-electron η^6 complexes. The sense of the distortion is that C_1 and C_4 in **2** move away from the metal towards a boat-shaped structure **3**. The distortion is small and exaggerated in **3**; nonetheless it is a definite feature. On the other hand, the 17-electron complex (π-tol)$Co(C_6F_5)_2$ contains a planar η^6-arene ligand.[3b] A preliminary theoretical discussion of this

(1) (a) University of North Dakota. (b) University of Houston. (c) Camille and Henry Dreyfus Teacher-Scholar, 1979–1984.
(2) Anderson, B. B.; Behrens, C. B.; Radonovich, L. J.; Klabunde, K. J. *J. Am. Chem. Soc.* **1976**, *98*, 5390.
(3) (a) Klabunde, K. J.; Anderson, B. B.; Bader, M.; Radonovich, L. J. *J. Am. Chem. Soc.* **1978**, *100*, 1313. (b) Radonovich, L. J.; Klabunde, K. J.; Behrens, C. B.; McCollar, D. P.; Anderson, B. B. *Inorg. Chem.* **1980**, *19*, 1221.
(4) Muetterties, E. L.; Bleeke, J. R.; Sievert, A. C. *J. Organomet. Chem.* **1979**, *178*, 197 and references therein.
(5) (a) Browning, J.; Green, M.; Penfold, B. R.; Spencer, J. L.; Stone, F. G. A. *J. Chem. Soc., Chem. Commun.* **1973**, 31. Browning, J.; Penfold, B. R. *J. Cryst. Mol. Struct.* **1974**, *4*, 335. Cobbledick, R. E.; Einstein, F. W. B. *Acta Crystallogr., Sect. B* **1978**, *B34*, 1849. Brauer, D. J.; Krüger, C. *Inorg. Chem.* **1977**, *16*, 884. (b) Timms, P. L; King, R. B. *J. Chem. Soc., Chem. Commun.* **1978**, 898. Darensbourg, M. Y.; Muetterties, E. L. *J. Am. Chem. Soc.* **1978**, *100*, 7425. Dickson, R. S.; Wilkinson, G. *J. Chem. Soc.* **1964**, 2699. Kang, J. W.; Childs, R. F.; Maitlis, P. M *J. Am. Chem. Soc.* **1970**, *92*, 720. Albright, J. O.; Datta, S.; Dezube, B.; Kouba, J. K.; Marynick, D. S.; Wreford, S. S.; Foxman, B. M. *Ibid.* **1979**, *101*, 611. Huttner, G.; Lange, S.; Fischer, E. O. *Angew. Chem., Int. Ed. Engl.* **1971**, *10*, 556. Huttner, G.; Lange, S. *Acta Crystallogr. Sect. B* **1972**, *B28*, 2049. Churchill, M. R.; Mason, R. *Proc. R. Soc. London, Ser. A* **1966**, *61*, 292. Band, A.; Bottril, M.; Green, M.; Welch, A. J. *J. Chem. Soc., Dalton Trans.*, **1977**, 2372. Herbstein, F. H.; Reisner, M. G. *J. Chem. Soc., Chem. Commun.* **1972**, 1077. Barlex, D. M.; Evans, J. A.; Kemmitt, R. D. W.; Russell, D. R. *Ibid.* **1971**, 331. Lucherine, A.; Porri, L. *J. Organomet. Chem.* **1978**, *155*, 45C.
(6) (a) Nolte, M. J.; Gafner, G.; Haines, L. *Chem. Commun.* **1969**, 1406. Nolte, M. J.; Gafner, G. *Acta Crystallogr., Sect. B* **1974**, *B30*, 738. (b) Schmidt, H.; Ziegler, M. L. *Chem. Ber.* **1976**, *109*, 132.

0020-1669/80/1319-3373$01.00/0

2 3

phenomenon in regard to rotational barriers has been given elsewhere.[7] Herein we shall compare the structural features of a series of (π-arene)ML_2 complexes and it will be shown that not only the puckering of the arene but also the arene to ML_2 distance varies in a predictable manner as a function of the electron count in the complex. Finally, a theoretical discussion of puckering in a related class of π-arene–ML_4 complexes[8] will be given.

Experimental Section

The crystal used for data collection, having dimensions 0.33 × 0.50 × 0.30 mm, was wedged in a glass capillary with the longest dimension parallel to the capillary wall. Precession photographs provided systematic absences consistent with $P2_1/n$. Structure analysis was continued in this space group because of the convenience of the β angle. Final lattice constants, determined on the diffractometer (λ = 0.709 26 Å) from 15 reflections centered at their positive and negative 2θ's, were a = 8.556 (1) Å, b = 19.125 (3) Å, c = 12.135 (3) Å, and β = 86.60 (2)°. This unit cell containing four molecules of η^6-$C_6H_3(CH_3)_3Ni(C_6F_5)_2$ provided a calculated density of 1.72 g/cm^3.

Intensity data were collected on a Picker FACS-I diffractometer with Zr-filtered Mo Kα radiation (λ = 0.7107 Å). With use of a takeoff angle of ~2$^1/_2$°, each peak was scanned 1.3° in 2θ plus a small increment for spectral dispersion at the rate of 1°/min. Background counts were of 20-s duration, and attenuators were inserted automatically when the count rate exceed ~10 000 counts/s. Data were collected to a limiting 2θ of 54.87°, and the laboratory temperature was maintained at 22 ± 1 °C. A set of three standard reflections, monitored after every 100 data, showed a small decrease of 5% over the course of data collection.

The linear adsorption coefficient[9] was 1.10 mm^{-1}, and an approximate calculation of transmission factors suggests the maximum error introduced on F from ignoring adsorption effects would be ~4%. Thus the data were directly reduced to a set of $|F_o|$'s by application of Lorentz and polarization corrections (Lp). Some 3279 data having $F_o > 2\sigma_F$ were taken as observed and utilized in the structure determination. Standard deviations were calculated as $\sigma_F = [(C + k^2B)/4|F_o|^2(Lp)^2]^{1/2}$ where C and B are the count of the scan and background, respectively, and k is the ratio of scan to background counting time.

The position of the Ni atom was located from a Patterson[10] synthesis, and all other atoms, except hydrogen, were located from subsequent Fourier[10] maps. Several cycles of full-matrix isotropic refinement[11] followed by block-diagonal refinement[12] with each atom treated anisotropically produced an R value of 6.97%, where $R = \sum||F_o| - |F_c||/\sum|F_o|$. Coordinates for the three aromatic hydrogens were obtained from a difference synthesis and included in further refinement along with anomalous dispersion corrections[13] for the Ni atom. This unit-weighted refinement produced an R value of 6.38% and R_w of 6.43%.

Empirical weights ($w = 1/\sigma^2$) were then calculated as described previously[3b] and used in the final cycles of refinement. A final R value of 6.37% and an R_w of 6.15% were produced. The data to parameter ratio was 11:1, and the error of fit was 1.47. A final difference map showed a residual electron density of 0.524 e/Å^3. The final atomic coordinates are listed in Table I, and the associated anisotropic thermal parameters are given in Table II.

Table I. Atomic Coordinates[a]

atom	10^4x	10^4y	10^4z
Ni	3098.9 (7)	3253.3 (3)	3386.6 (5)
C_1	1992 (5)	2494 (2)	2804 (4)
C_2	2713 (6)	1947 (2)	2252 (4)
C_3	1938 (6)	1354 (2)	1941 (4)
C_4	369 (6)	1301 (2)	2167 (4)
C_5	−411 (5)	1839 (3)	2705 (4)
C_6	402 (5)	2413 (2)	3012 (4)
F_2	4281 (4)	1960 (2)	2023 (4)
F_3	2690 (4)	829 (2)	1404 (3)
F_4	−398 (4)	715 (2)	1903 (3)
F_5	−1970 (3)	1775 (2)	2958 (3)
F_6	−428 (3)	2917 (2)	3570 (3)
C_7	2760 (6)	3810 (2)	2123 (4)
C_8	3732 (7)	3797 (3)	1188 (5)
C_9	3599 (9)	4277 (4)	319 (5)
C_{10}	2470 (9)	4770 (3)	394 (5)
C_{11}	1486 (8)	4794 (3)	1290 (6)
C_{12}	1637 (7)	4316 (3)	2130 (5)
F_8	4906 (5)	3317 (2)	1075 (3)
F_9	4656 (6)	4244 (3)	−562 (3)
F_{10}	2407 (7)	5231 (2)	−441 (4)
F_{11}	387 (6)	5304 (2)	1380 (4)
F_{12}	620 (4)	4385 (2)	3023 (3)
C_{13}	2749 (5)	3787 (2)	5017 (4)
C_{14}	3972 (5)	4088 (2)	4354 (4)
C_{15}	5294 (6)	3704 (2)	3942 (4)
C_{16}	5359 (6)	2996 (3)	4193 (5)
C_{17}	4091 (6)	2668 (2)	4766 (4)
C_{18}	2815 (6)	3074 (3)	5170 (4)
C_{19}	1380 (6)	4224 (3)	5489 (5)
C_{20}	6608 (6)	4061 (3)	3266 (6)
C_{21}	4127 (8)	1879 (3)	4979 (6)
H_{14}	3901 (61)	4540 (28)	4119 (43)
H_{16}	6179 (58)	2760 (28)	3865 (42)
H_{18}	2056 (61)	2882 (28)	5516 (42)

[a] Estimated standard deviations are given in parentheses.

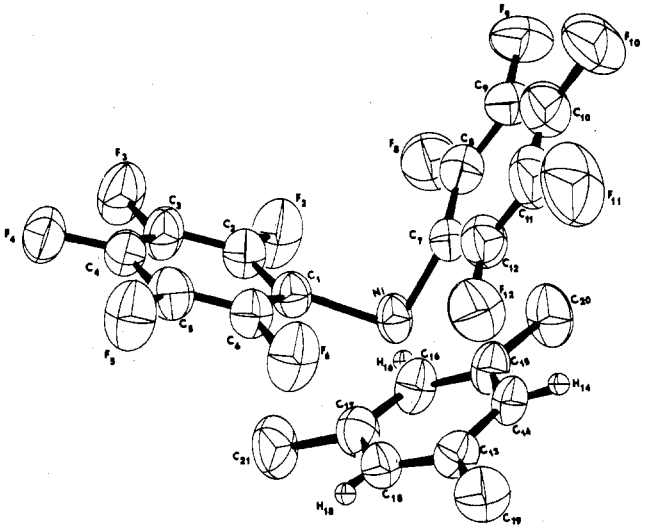

Figure 1. Traced ORTEP drawing of η^6-$C_6H_3(CH_3)_3Ni(C_6F_5)_2$. Ellipsoids are represented at 50% probability except for the H atoms which were deliberately reduced for clarity. The atomic numbering scheme is also given.

Discussion

A traced computer drawing of **1** is given in Figure 1. The thermal parameters in Table II are represented by ellipsoids drawn at 50% probability except for the hydrogens which were

(7) Albright, T. A.; Hoffmann, R.; Tse, Y.-C.; D'Ottavio, T. *J. Am. Chem. Soc.* **1979**, *101*, 3812.
(8) (a) Silverthorn, W. E.; Couldwell, C.; Prout, K. *J. Chem. Soc., Chem. Commun.* **1978**, 1009. (b) Atwood, J. L.; Hunter, W. E.; Rogers, R. D.; Carmona-Guzman, E.; Wilkinson, G. *J. Chem. Soc., Dalton Trans.* **1979**, 1519.
(9) MacGillavry, C. H., Rieck, G. D., Lonsdale, K., Eds., "International Tables for X-Ray Crystallography"; Kynoch Press: Birmingham, England, 1962; Vol. III.
(10) A. Zalkin's Fourier program FORDAP was used. Atomic form factors for nonhydrogen atoms were from: Cromer, D. T.; Mann, J. L. *Acta Crystallogr., Sect. A* **1968**, *A24*, 321.
(11) Busing, W. R.; Martin, K. O.; Levy, H. A. Report No. ORNL-TM-305, "OR-FLS, a Fortran Crystallographic Least Squares Program"; Oak Ridge National Laboratory: Oak Ridge, Tenn., 1962.
(12) The program REFINE by J. J. Park was used. The function minimized was $\sum w(|F_o| - |F_c|)^2$ where w is the weighting factor.
(13) Cromer, D. T.; Liberman, D. *J. Chem. Phys.* **1970**, 53, 1891.

Table II. Thermal Parameters (A^2) of the Atoms[a,b]

atom	B_{11}	B_{22}	B_{33}	B_{12}	B_{13}	B_{23}
Ni	3.71 (2)	2.93 (2)	5.13 (3)	−0.02 (2)	0.28 (2)	−0.28 (2)
C_1	4.2 (2)	3.0 (2)	4.8 (2)	0.1 (2)	−0.0 (2)	−0.2 (2)
C_2	4.1 (2)	4.3 (2)	6.1 (3)	−0.0 (2)	0.7 (2)	−0.7 (2)
C_3	5.2 (2)	3.4 (2)	6.0 (3)	0.2 (2)	0.4 (2)	−1.0 (2)
C_4	5.6 (3)	3.6 (2)	4.6 (2)	−0.7 (2)	−0.9 (2)	−0.2 (2)
C_5	3.7 (2)	4.5 (2)	6.0 (3)	−0.2 (2)	−0.4 (2)	−0.1 (2)
C_6	3.7 (2)	3.8 (2)	5.6 (3)	0.4 (2)	−0.2 (2)	−0.2 (2)
F_2	4.9 (1)	5.9 (2)	12.3 (3)	−0.8 (1)	2.6 (2)	−3.5 (2)
F_3	6.9 (2)	4.9 (2)	9.9 (2)	−0.3 (1)	1.6 (2)	−3.2 (2)
F_4	7.0 (2)	4.6 (1)	7.3 (2)	−1.5 (1)	−1.4 (1)	−1.1 (1)
F_5	3.9 (1)	6.3 (2)	11.5 (2)	−0.4 (1)	−0.2 (1)	−1.3 (2)
F_6	4.3 (1)	5.0 (1)	10.7 (2)	0.8 (1)	0.8 (1)	−2.1 (2)
C_7	5.9 (3)	3.5 (2)	4.7 (2)	−1.2 (2)	0.1 (2)	−0.1 (2)
C_8	8.1 (4)	4.8 (3)	5.9 (3)	−1.4 (2)	0.2 (3)	−0.8 (2)
C_9	11.0 (5)	7.4 (4)	4.1 (3)	−4.0 (3)	0.1 (3)	−0.2 (2)
C_{10}	11.7 (5)	5.6 (3)	6.3 (3)	−2.0 (3)	−2.7 (3)	1.4 (2)
C_{11}	8.5 (4)	4.9 (3)	8.4 (4)	−0.5 (3)	−2.5 (3)	−1.2 (3)
C_{12}	6.0 (3)	4.1 (2)	6.2 (3)	−0.3 (2)	−1.1 (2)	0.5 (2)
F_8	9.8 (2)	7.2 (2)	7.8 (2)	0.2 (2)	3.4 (2)	−1.0 (2)
F_9	17.3 (4)	11.0 (3)	5.9 (2)	−5.4 (3)	2.4 (2)	−0.8 (2)
F_{10}	18.4 (4)	9.4 (3)	8.4 (3)	−4.2 (3)	−5.1 (3)	4.3 (2)
F_{11}	11.7 (3)	6.7 (2)	13.4 (3)	0.8 (2)	−4.7 (3)	3.2 (2)
F_{12}	5.7 (2)	5.7 (2)	9.3 (2)	1.2 (1)	0.0 (1)	1.0 (2)
C_{13}	3.7 (2)	4.2 (2)	4.7 (2)	−0.0 (2)	−0.1 (2)	−0.7 (2)
C_{14}	3.9 (2)	3.0 (2)	5.7 (3)	0.0 (2)	−0.3 (2)	−0.7 (2)
C_{15}	3.7 (2)	4.0 (2)	6.2 (2)	−0.0 (2)	−0.2 (2)	−0.6 (2)
C_{16}	3.8 (2)	4.3 (2)	7.1 (3)	0.8 (2)	−0.4 (2)	−0.8 (2)
C_{17}	5.7 (3)	3.3 (2)	6.0 (3)	0.3 (2)	−1.0 (2)	0.2 (2)
C_{18}	4.6 (2)	4.4 (2)	5.3 (3)	−0.5 (2)	0.0 (2)	0.2 (2)
C_{19}	4.8 (3)	5.8 (3)	6.8 (3)	1.2 (2)	1.6 (2)	−1.0 (2)
C_{20}	4.0 (2)	5.8 (3)	9.9 (4)	−1.0 (2)	1.7 (2)	−0.0 (3)
C_{21}	9.2 (4)	3.3 (2)	9.1 (4)	0.4 (2)	−0.6 (3)	0.9 (2)

[a] Estimated standard deviations are given in parentheses. $B_{ij} = 4\beta_{ij}/a^*_i a^*_j$, where β_{ij} are the unitless parameters used in refinement in the form $\exp[-(\beta_{11}h^2 + \beta_{22}k^2 + \beta_{33}l^2 + 2\beta_{12}hk + 2\beta_{13}hl + 2\beta_{23}kl)]$. [b] Isotropic thermal parameters of the aromatic H atoms were fixed at 7 A^2.

Table III. Bond Distances (Å) within the Ligands

Pentafluorophenyl Rings					
C_1–C_2	1.368 (4)	C_9–C_{10}	1.349 (8)	C_5–F_5	1.356 (4)
C_2–C_3	1.379 (5)	C_{10}–C_{11}	1.336 (7)	C_6–F_6	1.354 (4)
C_3–C_4	1.358 (5)	C_{11}–C_{12}	1.379 (6)	C_8–F_8	1.362 (5)
C_4–C_5	1.372 (5)	C_{12}–C_7	1.365 (5)	C_9–F_9	1.360 (5)
C_5–C_6	1.364 (5)	C_2–F_2	1.354 (4)	C_{10}–F_{10}	1.347 (5)
C_6–C_1	1.378 (4)	C_3–F_3	1.341 (4)	C_{11}–F_{11}	1.355 (6)
C_7–C_8	1.367 (5)	C_4–F_4	1.346 (4)	C_{12}–F_{12}	1.355 (5)
C_8–C_9	1.407 (6)				
Mesitylene Ring					
C_{13}–C_{14}	1.405 (5)	C_{17}–C_{18}	1.404 (5)	C_{17}–C_{21}	1.533 (5)
C_{14}–C_{15}	1.415 (4)	C_{18}–C_{13}	1.378 (5)	C_{14}–H_{14}	0.91 (4)
C_{15}–C_{16}	1.389 (5)	C_{13}–C_{19}	1.522 (5)	C_{16}–H_{16}	0.91 (3)
C_{16}–C_{17}	1.402 (5)	C_{15}–C_{20}	1.514 (5)	C_{18}–H_{18}	0.84 (4)

deliberately reduced for clarity. Bond distances and angles are listed in Tables III and IV with estimated standard deviations (esd's) given in parentheses. Because block diagonal refinement was used, esd's were calculated by using only those terms involving positional parameters and are, therefore, underestimated.

Carbon atoms in the pentafluorophenyl ligands are planar, with the largest deviation being 0.008 Å and the average 0.004 Å. The average C–C distance of 1.369 (6) Å and C–F distance of 1.353 (5) Å are similar to those reported previously for the pentafluorophenyl group.[3b]

Bond parameters within the coordination sphere are given in Figure 2. The average Ni–C_σ bond length of 1.898 (4) Å is shorter than estimates of "normal" Ni–C_σ single-bond values.[14] Although this distance is slightly longer than that observed in the toluene complex (see Table V), the difference is only two esd's. The Ni–C_π bonds and perpendicular Ni–ring

(14) Churchill, M. R. *Perspect. Struct. Chem.* **1970**, *3*, 91–164.

Table IV. Bond Angles (Deg)

$C_1C_2C_3$	123.6 (3)	$C_7C_8C_9$	122.6 (4)	$C_{13}C_{14}C_{15}$	122.8 (3)
$C_2C_3C_4$	119.5 (3)	$C_8C_9C_{10}$	119.6 (4)	$C_{14}C_{15}C_{16}$	118.0 (3)
$C_3C_4C_5$	119.2 (3)	$C_9C_{10}C_{11}$	119.5 (4)	$C_{15}C_{16}C_{17}$	120.3 (3)
$C_4C_5C_6$	119.5 (3)	$C_{10}C_{11}C_{12}$	119.8 (4)	$C_{16}C_{17}C_{18}$	119.3 (3)
$C_5C_6C_1$	123.6 (3)	$C_{11}C_{12}C_7$	124.2 (4)	$C_{17}C_{18}C_{13}$	122.5 (3)
$C_6C_1C_2$	114.6 (3)	$C_{12}C_7C_8$	114.2 (3)	$C_{18}C_{13}C_{14}$	116.6 (3)
$C_1C_2F_2$	120.0 (3)	$C_7C_8F_8$	120.3 (4)	$C_{18}C_{13}C_{19}$	122.0 (3)
$C_2C_3F_3$	121.7 (3)	$C_8C_9F_9$	118.6 (5)	$C_{14}C_{15}C_{20}$	120.7 (3)
$C_3C_4F_4$	120.3 (3)	$C_9C_{10}F_{10}$	117.8 (5)	$C_{16}C_{17}C_{21}$	120.1 (3)
$C_4C_5F_5$	119.0 (3)	$C_{10}C_{11}F_{11}$	119.4 (4)	$C_{13}C_{14}H_{14}$	120 (2)
$C_5C_6F_6$	116.7 (3)	$C_{11}C_{12}F_{12}$	116.3 (3)	$C_{15}C_{16}C_{16}$	115 (2)

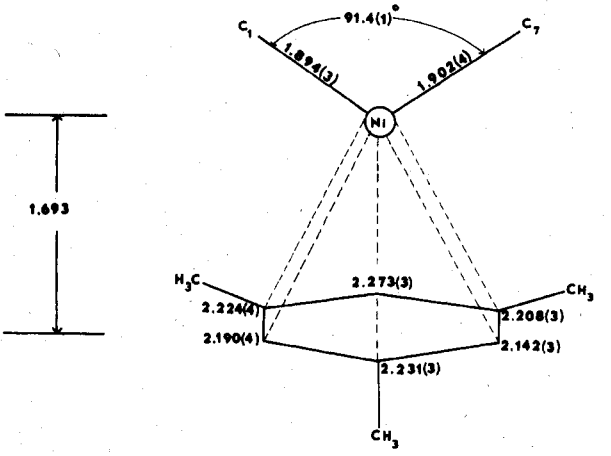

Figure 2. Bond parameters within the coordination sphere in η^6-$C_6H_3(CH_3)_3Ni(C_6F_5)_2$.

distances also show similar values between the two Ni(II) complexes. Thus, although the solution data[3a] indicate that electron-releasing ligands coordinate more strongly to Ni-

Table V. Comparison of Some Selected Bond Parameters in (arene)$M(C_6F_5)_2$ Complexes

	η^6-$C_6H_5CH_3$Co-$(C_6F_5)_2$[a]	η^6-$C_6H_5CH_3$Ni-$(C_6F_5)_2$[a]	η^6-$C_6H_3(CH_3)_3$-$Ni(C_6F_5)_2$[b]
M–C_σ, Å	1.931 (5)	1.891 (4)	1.898 (4)
M–C_π(av),[c] Å	2.141 (7)	2.192 (6)	2.211 (4)
r,[d] Å	1.627	1.681	1.693
θ,[e] deg	0	4.3	4.6

[a] Reference 3b. [b] This work. Esd's were calculated by using only those terms involving positional parameters, as obtained from block-diagonal refinement, and are underestimated relative to the other two structures which utilized the full variance–covariance matrix. [c] The average of the six M–C_π bonds. [d] r is the perpendicular distance from Co to the six-carbon plane and from Ni to the four-carbon plane. [e] θ is puckering angle of the two para carbons from the four-carbon mean plane.

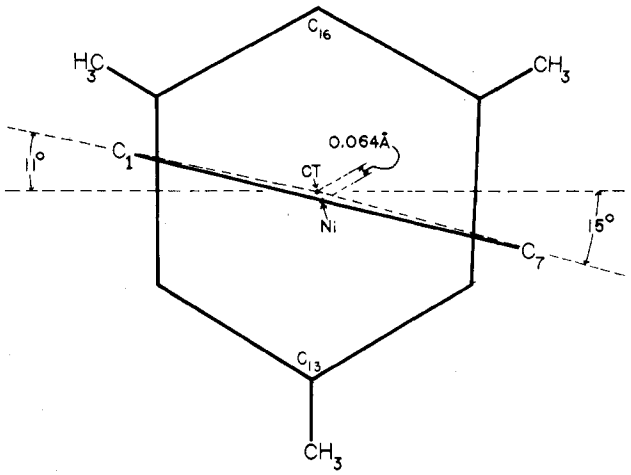

Figure 3. Orientation of the Ni and two σ-bonded carbons with respect to the η^6-mesitylene ligand. CT represents the center of the ring.

$(C_6F_5)_2$, no structural evidence of this is observed for the mesitylene complex. In fact, if the differences in Table V are real, they are in the opposite direction to what one would expect.

The carbon framework of the η^6-mesitylene ligand displays the same nonplanar geometry as that observed in the η^6-toluene complex (Table V). Accordingly C_{13} and C_{16} are bent 4.7 and 4.6°, respectively, from the mean plane of the other four carbons, away from the nickel. The perpendicular distance from the nickel to the four-carbon plane is 1.693 Å.

The orientation of the nickel atom and two σ-bonded carbons with respect to the π-mesitylene ligand is shown in Figure 3. It is somewhat different from that observed for the toluene complex. First, the mirror plane observed in the toluene complex that would include atoms corresponding to C_{16} and C_{13} is lost. In addition the nickel atom is displaced slightly by 0.06 Å from the perpendicular line passing through the ring center (CT). In the toluene complex the nickel atom is approximately on this line. The two σ-bonded carbons in the present structure are rotated by ~11 and ~15° from the horizontal plane bisecting the C_{14}–C_{15} and C_{17}–C_{18} bonds. In the toluene case this rotational angle is ~1° (due to the tilting of the two σ-bonded carbons away from the NiCT axis).[3b] These angles were approximated by deriving coordinates of an imaginary atom (PNi) lying on the perpendicular line through CT and calculating the angle between the horizontal plane and planes defined by C_7PNiCT and C_2PNiCT. This orientation minimizes intermolecular interactions with the shortest F···F distance of 2.89 Å occurring between F_{10}···F_{11}^{I} and the shortest C···F interaction of 2.95 Å between C_5···F_9^{II}, where I = $-x$, $1-y$, $-z$ and II = $-^1/_2+x$, $-^1/_2-y$, $^1/_2+z$. Rotation of the $Ni(C_6F_5)_2$ unit toward or further away from the horizontal plane results in more serious intermolecular interactions for a fixed rotation of the C_6F_5 group about the C_7–Ni and C_1–Ni bonds. The intermolecular interactions involving methyl carbons are all greater than normal van der Waals contact distances in the observed orientation. Thus the differences between the mesitylene and toluene structures could be the result of packing forces.

The important results in Table V are the following. On going from cobalt to nickel, for complexes of the type (η^6-arene)$M(C_6F_5)_2$, the M–C_π bond distances increase while the M–C_σ bond distances decrease. Second, the same "boat" deformation for the two-18-electron nickel complexes in the η^6-arene ligand are observed, while the arene is planar for the 17-electron species. The origin of these trends is electronic in nature. We now turn to a discussion of the bonding in these complexes.

A theoretical analysis of the bonding in the 17- and 18-electron complexes was carried out by means of extended Hückel calculations with geometrical details and parameters listed in the Appendix. Calculations for two types of ligands were done on the (benzene)ML_2 complexes. In the first case, L is a σ-donor group, modeled by a single s orbital. The optimized value of θ, defined again in **4**, was found to be 4°

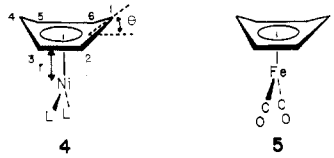

4 **5**

for an 18-electron benzene–NiL_2. Taking one electron out of the HOMO of **4** results in **4** preferring to remain planar (θ = 0°). Maintaining θ = 4° for the 18-electron complex, we found an optimimum value of r, the distance from the nickel to the plane defined by C_2, C_3, C_5, and C_6 to be 1.55 Å. The optimized value for r for the 17-electron complex (θ held at 0°) was found to be 1.49 Å. The degree of puckering, θ, is fairly close to the experimental values we have given previously. While r is calculated to somewhat shorter than the experimental values for the N(II) and Ni(III) complexes, the trend is in the right direction—r is considerably shorter for the 17-electron complex. Next, a series of calculations was carried out for when L is a π acceptor, namely, for $(C_6H_6)Fe(CO)_2$ (**5**). Here for the neutral 18-electron complex a planar structure is preferred. However, the bending force constant for puckering is quite low—it costs only 0.9 kcal/mol to distort to a structure with θ = 4°. The same distortion in 17-electron $(C_6H_6)Fe(CO)_2^+$ requires 1.9 kcal/mol. The optimized value of r for the 18-electron species is calculated to be 1.64 Å—a more realistic value. The value of r shrinks to 1.61 Å for the 17-electron complex.

For explanation of these results, the valence molecular orbitals of a $(C_6H_6)NiL_2$ complex can be derived from the interaction of the important valence orbitals of an ML_2 unit with the π orbitals of benzene. This is done in Figure 4 for a planar complex. We also are considering a conformation in **4** and **5** (analogous to the toluene complexes) where the ML_2 group bisects C_2–C_3 and C_5–C_6 bonds. Rotation from this by 10° to that in the mesitylene complex will not change the qualitative features. The valence orbitals of an ML_2 fragment have been extensively discussed elsewhere.[15] Basically there is a

(15) (a) Hofmann, P. *Angew. Chem.* **1977**, *89*, 551; Halibitation, Universität Erlangen, 1978. (b) Albright, T. A.; Hoffmann, R. *Chem. Ber.* **1978**, *111*, 1578. (c) Albright, T. A.; Hoffmann, R.; Thibeault, J. C.; Thorn, D. L. *J. Am. Chem. Soc.* **1979**, *101*, 3801. (d) Elian, M.; Hoffmann, R. *Inorg. Chem.* **1975**, *14*, 1058. (e) Burdett, J. K. *Ibid.* **1975**, *14*, 375; *J. Chem. Soc., Faraday Trans. 2* **1974**, *70*, 1599. (f) Mingos, D. M. P. *J. Chem. Soc., Dalton Trans.* **1977**, 602; *Adv. Organomet. Chem.* **1977**, *15*, 1.

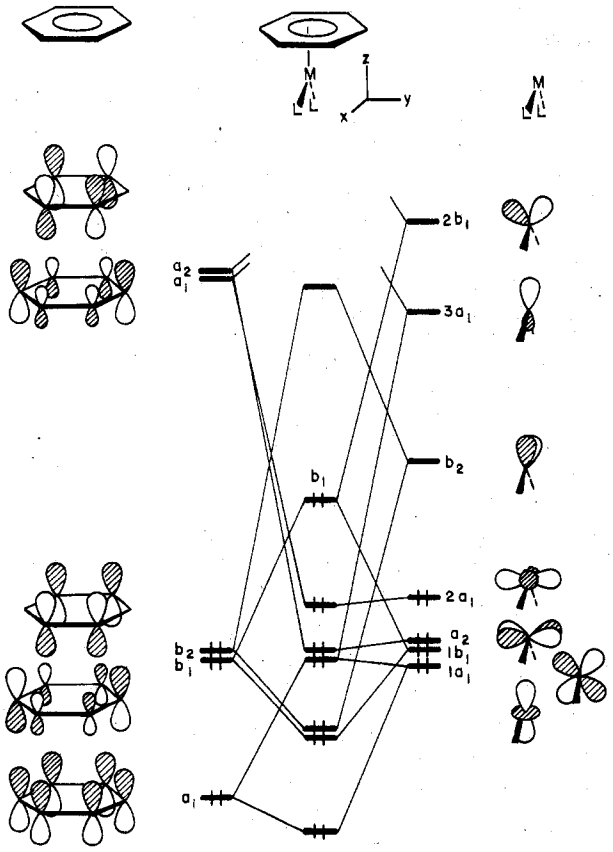

Figure 4. Interaction diagram for (benzene)ML_2. The electron count is appropriate for an 18-electron complex.

nest of four nonbonding orbitals at low energy. With use of the coordinate system given in Figure 4, these are z^2, yz, xy, and $x^2 - y^2$. These transform as $1a_1$, $1b_1$, a_2, and $2a_1$ in the C_{2v} geometry of the molecule. At higher energy, the LUMO of a d^8 system, e.g., Ni(II) or Fe(0), is b_2. This is an orbital of metal xz and x character and is hybridized out away from the metal.[15] At high energy there remain $3a_1$ and $2b_1$. $3a_1$ is mainly metal s, z, and z^2. The energy and composition of $2b_1$ depend on the electronic nature of the L groups. When L is a π acceptor like CO, $2b_1$ lies at relatively low energy, close to that of $3a_1$ from our calculations. It is primarily carbonyl π^* in character, antibonding with respect to metal yz and bonding to metal y.[15a] This is shown by **6**. The final,

6

hybridized shape of $2b_1$ is again directed away from the metal. When L is a σ donor with no π-bonding capabilities, $2b_1$ lies at much higher energy and is comprised primarily of metal y. Now $1a_1$ and $3a_1$ interact with the lowest a_1 π orbital of benzene to form three orbitals. The two lowest in energy and shown in Figure 4 are filled. The a_2 and $2a_1$ orbitals interact with benzene π^* in a bonding manner and are also destabilized by two ring orbitals, not shown in Figure 4 which are also of δ symmetry. Thus, a_2 and $2a_1$ stay at approximately the same energy. A very strong stabilizing interaction occurs between b_2 of ML_2 and the b_2 π orbital of benzene. Finally, and most importantly to our discussion, ML_2 $1b_1$ and benzene b_1 form a bonding and antibonding set, *both* of which are filled. The

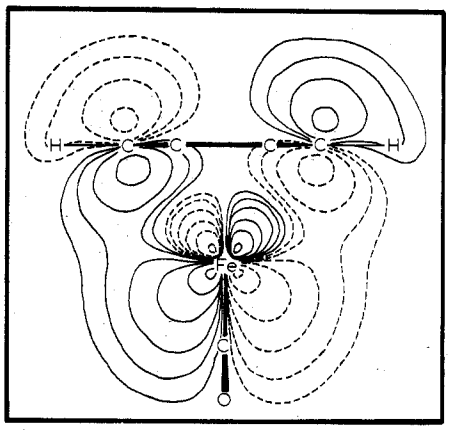

Figure 5. Plot of the HOMO in $(C_6H_6)Fe(CO)_2$. The values of ψ are ± 0.4, 0.2, 0.1, 0.05, 0.25, and 0.0125.

latter, labeled b_1 in the interaction diagram of Figure 4, is the HOMO of the molecule. It is drawn in **7**. The antibonding

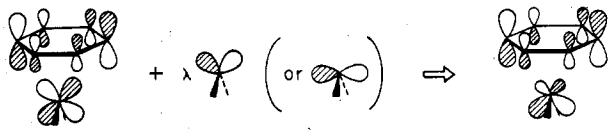

7 **8**

between C_1 and C_4 with $1b_1$ causes the ring to pucker. Removing one electron from **7** causes the driving force of the distortion to be lost. The same argument can be applied to the variation of r with respect to the occupancy of the molecular b_1 orbital. The antibonding of $1b_1$ in ML_2 with benzene b_1 can be and is moderated by the intervention of $2b_1$ on ML_2. This fragment orbital mixes into **7** in a bonding fashion, as shown in **8**. The magnitude of mixing coefficient, λ, depends primarily on the energy of $2b_1$. The lower $2b_1$ is in energy, the greater it mixes into the HOMO. Therefore, acceptor ligands will cause an increased amount of $2b_1$ to mix in. Our calculations reflect this. For $(C_6H_6)Fe(CO)_2$, the HOMO contains 15% of $2b_1$, and this diminishes to 5% for $(C_6H_6)NiL_2$. The structural consequence of increased $2b_1$ mixing is to abate the ring puckering (diminish θ) and decrease the difference of r with respect to its 17-electron counterpart. Nonetheless **8** is quite antibonding with respect to C_1 and C_4 even for $(C_6H_6)Fe(CO)_2$. This can be seen from a contour plot of **8** in Figure 5. The presence of the high-lying HOMO, b_1, also makes these compounds quite basic.[17]

It is difficult to decide how the effects of the substitution of π donor or acceptors on the arene ring will affect r and θ. The substitution of one good π donor or, better yet, two para π donors causes the energy of the benzene σ b_1 to raise. The most favorable conformation of the molecule is then **9**, rather

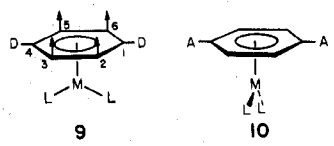

9 **10**

than **4**, as has been discussed previously.[7] The symmetry of the b_1 levels in ML_2 changes to b_2 and vice versa; therefore, the antibonding between it and the benzene π orbital of b_2 symmetry in Figure 4 causes C_2, C_3, C_5 and C_6 to move away from the metal. This indeed does happen in (benzene)ru-

(16) Throughout this paper we use the simplified notation z^2, $x^2 - y^2$, xz, and yz and xy, yz, and xy for the nd orbitals and x, y, and z for the $n + 1$ metal p orbitals.

(17) See, for example, the $(\eta^5\text{-Cp})CoL_2$ complexes which have an analogous HOMO: Werner, H.; Hofmann, W. *Angew. Chem.* **1977**, *89*, 835. Hofmann, W.; Buchner, W.; Werner, H. *Ibid.* **1977** *89*, 836 and references therein.

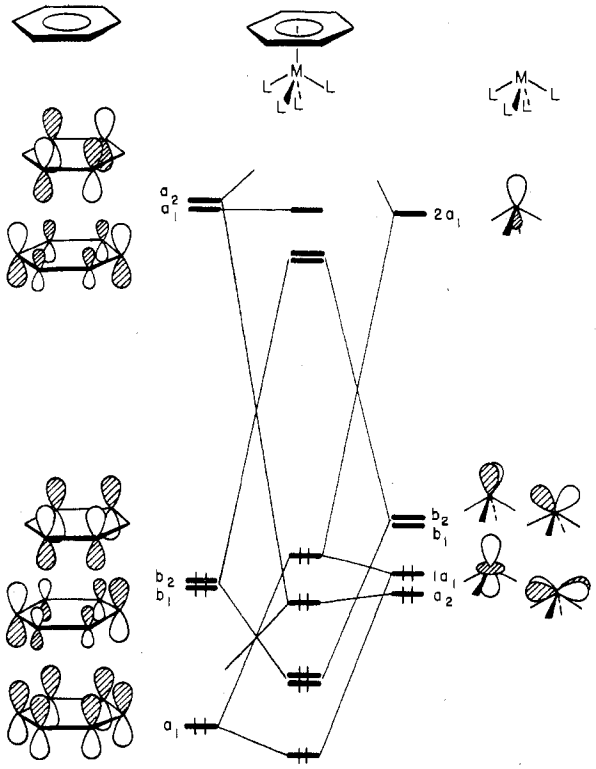

Figure 6. Interaction diagram for an 18-electron (benzene)ML_4 complex. The trans L–M–L angles are assumed to be equal.

thenium cyclooctadiene.[6b] One or two strong π acceptors substituted on the arene create a preference for the alternative conformation **10**; however, the energy gap between the benzene b_1 orbital and $1b_1$ will increase. The amount of mixing in the HOMO then decreases (b_1 will become more localized on the ML_2 portion), and again the tendency for distortion decreases. Relatively weak π acceptors or donors (as are methyl groups) should cause relatively minor effects. This appears to be the case in Table V.

The deformation of a η^6-coordinated arene to a boat structure has also been observed for three (arene)ML_4 complexes, **11–13**.[8] Compound **11** is diamagnetic and presumably

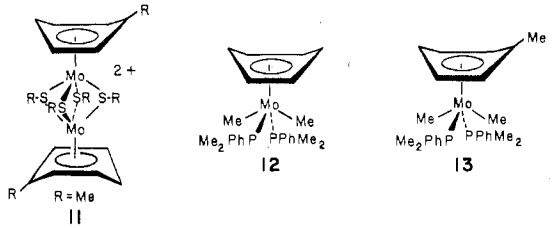

contains a Mo–Mo single bond; therefore, each complex contains a d^4 ML_4 fragment. Although steric interactions can be used to rationalize the deformation in **11–13**, we think that there is also an electronic driving force. We can construct an interaction diagram for a planar (benzene)ML_4 complex in a manner analogous to that presented before. This is done in Figure 6. There are two differences in the valence orbitals of an ML_4 fragment[15c,d] compared to ML_2. First, the b_1 and b_2 orbitals merge together in energy and hydridization until they become degenerate if both trans L–M–L angles are equal.[15c] Second, the $2a_1$ orbital in ML_2 is destabilized tremendously upon the introduction of two additional ligands. It is not shown in Figure 6. The b_2 and b_1 π orbitals of benzene form a strong bonding interaction with b_2 and b_1 of ML_4. The a_1 π level of benzene together with $1a_1$ and $2a_1$ in ML_4 create a set of three orbitals, two of which are filled for **12** and **13**.

Table VI. Parameters Used in the Extended Hückel Calculations

orbital	H_{ii}, eV	ξ_1	ξ_2	C_1	C_2
Ni 3d	−12.99	5.75	2.00	0.5682	0.6292
4s	−8.86	2.10			
4p	−4.90	2.10			
Fe 3d	−12.70	5.35	1.80	0.5366	0.6678
4s	−9.17	1.90			
4p	−5.37	1.90			
Cr 3d	−11.22	4.95	1.60	0.4876	0.7205
4s	−8.66	1.70			
4p	−5.24	1.70			
C 2s	−21.40	1.625			
2p	−11.40	1.625			
O 2s	−32.30	2.275			
2p	−14.80	2.275			
P 3s	−18.6	1.60			
3p	−14.0	1.60			
H 1s	−13.60	1.30			

This leaves us with the a_2 level of ML_4. It is slightly stablized by benzene a_2. The bonding interaction, **14**, causes a distortion

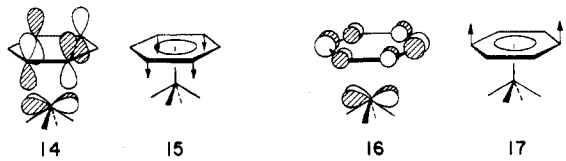

in the sense of **15**. Furthermore, a high-lying benzene σ orbital (one member of the e_{2g} set) also interacts with the ML_4 a_2. It does so in this level in an antibonding way, **16**, creating the distortion in **17**. Either or both of the distortions result in a boat structure for the coordinated arene. Our calculations on $(C_6H_6)CrMe_2(PH_3)_2$ and $(C_6H_6)Cr(PH_3)_4^{2+}$ clearly show this effect in that orbital given by the combination of **14** and **16**. The optimum value of θ (defined as in **4**) for the former compound was 7° and for the latter 6°. In **12–13** θ is in the range of 8–10°.[8b] The electronic situation for **11** is entirely analogous and will not be presented here.

Notice that in the ML_2 fragment there are two orthogonal δ-type orbitals—a_2 and $2a_1$. Each δ function acts in the same manner with the benzene π^* and $\sigma(e_{2g})$ sets to approximately the same extent. The arene ring then would remain planar if it were not for the $b_2 - 1b_1$ difference in ML_2. In the ML_4 complexes b_2 and b_1 are identical, and it is the δ set which creates the differentiation.

Other π-bonded ligands are capable of similar distortions. One established example which has been carefully analyzed by Byers and Dahl[18] is $Me_5C_5Co(CO)_2$. It is again the antibonding of $1b_1$ with one of the Cp π orbitals that causes, now, three carbons to move away from Co in the Cp ligand. In a hypothetical (cbd)$Ni(CO)_2$ (cbd = cyclobutadiene) molecule[19] we predict[7] that the cyclobutadiene ring should become rectangular if the $Ni(CO)_2$ orientation eclipses C–C bonds or the $Ni(CO)_2$ unit could adopt a η^2 geometry. If the most stable (η^4) $Ni(CO)_2$ conformation eclipses carbon atoms in the cyclobutadiene ligand then, again the two staggered carbons will pucker away from the nickel. In the ML_4 series there will be few examples of the distortion. (cbd)ML_4 complexes have planar, square geometries.[20] The a_2 orbital operates equivalently on four carbons of any π-bonded ligand.

Acknowledgment. T.A.A. thanks the Robert A. Welch Foundation and Research Corp. for generous support of this work. L.J.R. also wishes to acknowledge Research Corp. for generous support and the University of North Dakota for

(18) Byers, L. R.; Dahl, L. F. *Inorg. Chem.* **1980**, *19*, 277.
(19) An isoelectronic example recently prepared is cbdNi(bpy): Griebsch, U.; Hoberg, H. *Angew. Chem.* **1978**, *90*, 1014.
(20) Davis, Raymond, private communication. Oliver, J. D. Ph.D. Dissertation, University of Texas at Austin, 1971.

computer time. We also would like to thank B. B. Anderson and K. J. Klabunde for a sample of **1** and J. Atwood and R. Davis for unpublished results and communications.

Appendix

The calculations were carried out with the extended Hückel method.[21] The metal orbital H_{ii}'s and exponents were taken from previous work.[7] The parameters are listed in Table VI. The modified Wolfsberg–Helmholz formula was used.[22] The following idealized bond lengths were used: C–H = 1.09, C–C = 1.41, Fe–C = 1.78, C–O = 1.14, Cr–P = 2.37, P–H = 1.42, Cr–C = 2.20, and Ni– 1.60 Å. Regular bond angles in the benzene ligand were utilized; the rest were taken from the average of the available structures.[3b,8b] The C–Fe–C, Fe–C–O, L–Ni–L, and P–Cr–P angles were set at 88, 180, 88, and 120°, respectively. The parameters used for the L ligand in **4** were identical with those of H.

(21) Hoffmann, R. *J. Chem. Phys.* **1963**, *39*, 1397. Hoffmann, R.; Lipscomb, W. N. *Ibid.* **1962**, *36*, 3179, 3489; **1962**, *37*, 2872.
(22) Ammeter, J. H.; Bürgi, H. B.; Thibeault, J. C.; Hoffmann, R. *J. Am. Chem. Soc.* **1978**, *100*, 3686.

Registry No. **1**, 74153-73-4.

Supplementary Material Available: Listing of structure factor amplitudes (16 pages). Ordering information is given on any current masthead page.

Contribution from the Department of Chemistry, Columbia University, New York, New York 10027

Molecular Structure and Ligand-Exchange Reactions of Trichlorotris(*tert*-butyl isocyanide)vanadium(III). Synthesis of the Hexakis(*tert*-butyl isocyanide)vanadium(II) Cation

LANCE D. SILVERMAN, JOHN C. DEWAN, CHRISTEN M. GIANDOMENICO, and STEPHEN J. LIPPARD*

Received May 8, 1980

The reaction between vanadium(III) chloride and *tert*-butyl isocyanide is shown to produce *mer*-$VCl_3(CN\text{-}t\text{-}Bu)_3$ rather than an insertion product as claimed by previous investigators. The compound crystallizes in the trigonal crystal system, space group $P3_121$, with a = 11.765 (1) Å, c = 13.611 (2) Å, and Z = 3. The structure was determined by single-crystal X-ray diffraction methods and refined to R_1 = 0.048. The molecule has crystallographically required twofold symmetry. The V–Cl bond lengths are 2.288 (4) Å (unique) and 2.317 (2) Å, and the V–C bond lengths are 2.186 (15) Å (unique) and 2.189 (9) Å. These values indicate a slightly greater structural trans effect for chloride compared with that for isocyanide in this molecule. The preference for the meridional form is attributed to steric factors since even in this isomer the Cl–V–Cl bond angles open to 97.2 (1)° with a concomitant reduction in Cl–V–C to 82.8 (1)°. Proton NMR spectroscopic studies of paramagnetic *mer*-$VCl_3(CN\text{-}t\text{-}Bu)_3$ in deuterated chloroform revealed separate *tert*-butyl resonances of intensity ratio 2:1 that coalesce above 60 °C to a single peak. Addition of free isocyanide to $VCl_3(CN\text{-}t\text{-}Bu)_3$ at 33 °C produced selective exchange of the unique *tert*-butyl isocyanide ligand. This result shows that $Cl^- > CN\text{-}t\text{-}Bu$ in its kinetic trans effect. Trichlorotris(*tert*-butyl isocyanide)vanadium(III) reacts with 2,2′,2″-terpyridine to form VCl_3(terpy) and with excess *tert*-butyl isocyanide to yield the $[V(CN\text{-}t\text{-}Bu)_6]^{2+}$ cation. The latter is the first homoleptic isocyanide–vanadium complex and was also prepared directly from vanadium(III) chloride.

There are few literature reports of isocyanide complexes of vanadium. This situation is in marked contrast to the extensive and varied chemistry of the isocyanide complexes of Cr, Mo, and W[1] and presumably results from the lower thermal, hydrolytic, and oxidative stability of vanadium isocyanide complexes. The known vanadium isocyanide complexes include adducts with dicyclopentadienylvanadium[2] and reported insertion products of isocyanides with vanadium(III) chloride.[3] Structural data on these compounds have thus far been lacking.

In an extension of our synthetic, structural, and chemical studies of molybdenum and tungsten isocyanide complexes,[4] we have begun to explore vanadium isocyanide chemistry. Here we show that the previously reported "insertion" reaction,[3b] thought to yield **1**, in fact forms *mer*-$VCl_3(CNR)_3$, R = *tert*-butyl, **2**. We also describe the first homoleptic vanadium isocyanide complex, $[V(CNR)_6]^{2+}$, and the reaction of **2** with 2,2′,2″-terpyridine to produce VCl_3(terpy). Finally, proton NMR spectroscopic studies of paramagnetic *mer*-$VCl_3(CN\text{-}t\text{-}Bu)_3$ are reported that, together with IR spectra, establish its structure in solution and demonstrate the greater trans effect of chloride vs. *tert*-butyl isocyanide in promoting exchange of bound and free isocyanides.

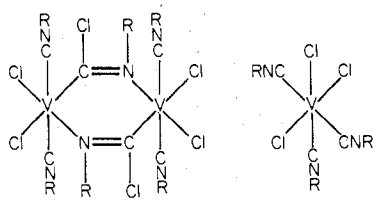

1 **2**

Experimental Procedure

Synthetic Work. All complexes were prepared and handled under an atmosphere of dry nitrogen with the use of Schlenk techniques or in a Vacuum Atmospheres drybox. *tert*-Butyl isocyanide was synthesized by a literature method.[5] All other starting materials were commercially available. Solvents were distilled from appropriate drying reagents, under nitrogen, immediately before use. Chemical analyses were performed by Galbraith Laboratories, Knoxville, Tenn.

(1) (a) Malatesta, L.; Bonati, F. "Isocyanide Complexes of Metals"; Wiley-Interscience: New York, 1969. (b) Lippard, S. J. *Prog. Inorg. Chem.* **1976**, *21*, 91.
(2) (a) Fachinetti, G.; Floriani, C. *J. Chem. Soc., Chem. Commum.* **1975**, 578. (b) Fachinetti, G.; Del Nero, S.; Floriani, C. *J. Chem. Soc., Dalton Trans.* **1976**, 1046. (c) Moise, C.; El Murr, N.; Rivecciê, M.; Tirouflet, J. *C. R. Hebd. Seances Acad. Sci., Ser. C* **1978**, *287*, 329.
(3) (a) Crociani, B.; Nicolini, M.; Richards, R. L. *J. Organomet. Chem.* **1975**, *101*, C1. (b) Behnam-Dehkordy, M.; Crociani, B.; Nicolini, M.; Richards, R. L. *Ibid.* **1979**, *181*, 69.
(4) (a) Dreyer, E. B.; Lam, C. T.; Lippard, S. J. *Inorg. Chem.* **1979**, *18*, 1904. (b) Lam, C. T.; Novotny, M.; Lewis, D. L.; Lippard, S. J. *Ibid.* **1978**, *17*, 2127. (c) Lam, C. T.; Corfield, P. W. R.; Lippard, S. J. *J. Am. Chem. Soc.* **1977**, *99*, 617 and references cited therein.
(5) Weber, W. P.; Gokel, G. W.; Ugi, I. K. *Angew. Chem., Int. Ed. Engl.* **1972**, *11*, 530.

0020-1669/80/1319-3379$01.00/0